Destruction of Freons by the Use of High-Voltage Glow Plasmas

Franz-Josef Spiess,[†] Xiao Chen,[†] Stephanie L. Brock,[†] Steven L. Suib,*[,†,‡,§] Yuji Hayashi,[||] and Hiroshige Matsumoto[⊥]

U-60, Department of Chemistry, Department of Chemical Engineering and Institute of Materials Science, University of Connecticut, Storrs, Connecticut 06269-3060, Nagasaki University, Nagasaki, 852 Japan, and Fujitsu Laboratories Ltd., Kawasaki, 852 Japan

Received: June 12, 2000; In Final Form: August 14, 2000

The decomposition of two different Freon species, Freon 21 ($CHFCl_2$) and Freon 142-B (CF_2ClCH_3), was carried out using a high-voltage glow discharge plasma. The plasma is produced in a tubular reactor consisting of an inner iron electrode and an outer electrode being either aluminum or copper, a glass tube between the electrodes serves as a dielectric. The reaction gases, 0.5% Freon in helium and 5% oxygen in helium (moisture added), are mixed on line. The conversion measured by a gas chromatograph as the disappearance of the Freon species is very high for both species. For Freon 21, the conversion ranges from 75% up to 100% in the input voltage regime between 1.60 and 5.44 kV depending on the mixture. In the case of Freon 142 B, higher voltages are needed to achieve similar conversions. The input voltage of 3.50 kV yields 70% conversion, 3.88 kV yields 77% conversion, and 5.44 kV gives 100%. The conversion of Freon 21 drops with increasing flow rate and decreases from 88% at 15 mL/min to 78% at 40 mL/min and to 47% at 100 mL/min. A more drastic decrease is seen with respect to CO_2 production, which decreases by 30% when the flow rate is changed from 20 to 40 mL/min and by 42% if changed to 60 mL/min. Oxygen increases CO_2 production via breakdown of Freon by 90%. Further addition of water increases CO_2 production by another 25% compared to the reaction with oxygen. Carbon dioxide is the main carbon oxide produced at a CO/CO_2 ratio of 0.05 to 0.07. Further reaction products are hydrogen fluoride and chlorine. Furthermore, mass spectroscopic and optical emission studies were carried out to obtain insight on the reaction mechanism.

Introduction

Freons, better known as **C**hloro**F**luoro**C**arbons (**CFC**s), are volatile organic compounds (VOCs) that have been used as propellants in aerosol sprays, refrigerants, solvents in the electronic industry, as well as foam blowing agents. Due to their inertness and lack of reactivity, they get slowly transported into the stratosphere over many years where they undergo photochemical reactions.[1] These photochemical reactions are yielding species that are involved in the destruction of the ozone layer. Most of the photochemically produced chlorine radicals end up as hydrogen chloride or chlorine nitrate, the so-called "reservoir species".[2,3] These decompose providing small amounts of catalytically active atomic chlorine and chlorine monoxide. Each chlorine atom introduced into the stratosphere destroys thousands of ozone molecules before removal. The less abundant bromine is 10−100 times more destructive than chlorine and does not have a "reservoir. The chemistry of ozone destruction is very complicated.[4]

The Freons used in these experiments are actually hydrochorofluorocarbons (HCFCs), Freon 21 (dichlorofluoromethane) and Freon 142B (1-chloro-1,1-difluoroethane). They contain a certain amount of hydrogen atoms. These molecules replaced CFCs as refrigerants. They are more readily attacked by the hydroxyl radical, therefore significantly reducing their amount reaching the stratosphere. Their potential to destroy ozone is just 1 to 10% of that of CFC-12, a standard for ozone depletion, and is even smaller for hydrofluorocarbons (HFCs).[5] The short- and long-term effects of these species are disputed.[6] Studies done by Hayman et al.[7] indicate a very low effect of these compounds in ground-level ozone formation, but due to their stability they have a high global warming potential and contribute to the stratospheric ozone depletion. Starting in 1985, several international conferences were held. In 1987, the primary international agreement, the Montreal Protocol, provided control measures on the production and consumption of ozone-depleting species. As of February 2000, 173 countries have ratified the Protocol that was amended several times, latest in 1997.[8]

Traditionally, thermal methods, such as incineration and thermal plasmas, were used to achieve "cleaner" products but installation costs are high and toxic exhaust gases are formed.[9,10] Catalytic oxidation and adsorption are problematical due to deactivation and poisoning of the catalyst.[10] Takita et al.[11] found promising results for the decomposition of CCl_2F_2 and CH_2FCF_3 involving water and oxygen. Furthermore, electrochemical methods proved to be highly efficient in the destruction of CFC-12 and 13.[12,13]

Recently, the focus for VOC removal shifted to nonthermal plasmas. Nonthermal plasmas are distinguished between microwave (MW) and electronic plasmas. MW plasmas are used in the power regime of a hundred kilowatts to several megawatts and at variable low pulse rates under low pressure. Gritsinin et al.[14] found that effective MW destruction of CCl_2F_2 occurs

* Author to whom correspondence should be addressed.
[†] Department of Chemistry, University of Connecticut.
[‡] Department of Chemical Engineering, University of Connecticut.
[§] Institute of Materials Science, University of Connecticut.
[||] Fujitsu Laboratories, Ltd.
[⊥] Nagasaki University.

10.1021/jp0021190 CCC: $19.00
Published on Web 11/01/2000

forming fluorine-rich species such as CF_4 and CF_3Cl, and postulated a mechanism involving chemical transformations and photodissociation. Aleksandrov et al.[15] showed that a plasma catalytic cycle employing electrons and negative ions in the decomposition of CCl_4 in humid air in a MW discharge afterglow reduces energy expense.

Electronic plasmas can be classified by the frequency used to drive the discharge and the type of discharge itself. RF discharge plasmas have to be discerned from surface, silent, and glow discharge plasmas. Radio frequency (RF) plasmas favor electron impact dissociation over electron attachment dissociation as Stoffels et al.[16] observed for dissociation of CCl_2F_2 (up to 90%) at low pressure (0−400 mTorr) and high power input. Wang et al.[17] showed for the same compound that high decomposition rates (up to 94%) and high selectivities to CH_4 and C_2H_2 (up to 80%) are achievable in a low-pressure hydrogen−argon RF plasma system. A dielectric barrier discharge at low frequency was used by Korzekwa et al.[18] to decompose a mixture of volatile organic compounds (VOCs) including Freons at atmospheric pressure.

Surface discharge investigation of CFC-113 in air at atmospheric pressure by Oda et al.[19] showed high concentrations of intermediate halogenated carbons and hydrocarbons at low decomposition rates, and HCl, CO_2, and N_2O at higher rates as products. The same authors found that the power efficiency does not differ between a ceramic, a coil type, and a coaxial reactor, but peak voltage does slightly.[20] Akhmedzhanov et al.[21] found trends similar to Stoffels' work[16] for CFC-113 favoring electron impact and collisions at high content and dissociative attachment at lower content. For laser sparks and slipping surface discharge treatment of CF_2Cl_2 a reaction scheme similar to the one for a MW plasma by Gritsinin[14] was proposed by Akhvlediani et al.[22] but photodissociation was not involved.

In our case glow plasma decomposition of HCFC-21 and 142B was investigated and a mechanism for these decompositions is being proposed using optical emission and mass spectrometry results. Furthermore, the influences of factors such as input voltage and flow rate were studied, and power consumption and efficiencies are discussed in this paper. The reactor employed in this case is a coaxial reactor favoring silent discharges.[20]

Experimental Section

Preparation of Gas Mixtures. A 1.0% mixture of Freon 21 in helium was prepared by mixing 1.5 psia Freon 21 (98% purchased from Aldrich Chemicals) with helium UHP (Ultrahigh Purity, from Connecticut Airgas) to achieve a total pressure of 150 psia. The 0.5% mixture of Freon 142 B in helium was prepared accordingly. A 10% mixture of oxygen in helium was used as obtained from Connecticut Airgas.

Plasma Reactor. The reactions involving Freon destruction were carried out in a Plasma and Catalysis Integrated Technologies (PACT) tubular type reactor. The reactor consists of three parts. The inner electrode is an iron rod of 9.50 mm diameter. A Pyrex glass tube of 9.91 mm i.d. and 11.89 mm o.d. for earlier experiments and later a quartz tube of the same dimensions were used to separate the inner from the outer electrode as the dielectric. The outer electrode is wrapped around the glass tube and is subsequently wrapped with copper wire to achieve a close coverage of the glass tube in order to achieve uniform plasmas. Aluminum and copper foil of 19.7 cm length are used for this purpose.

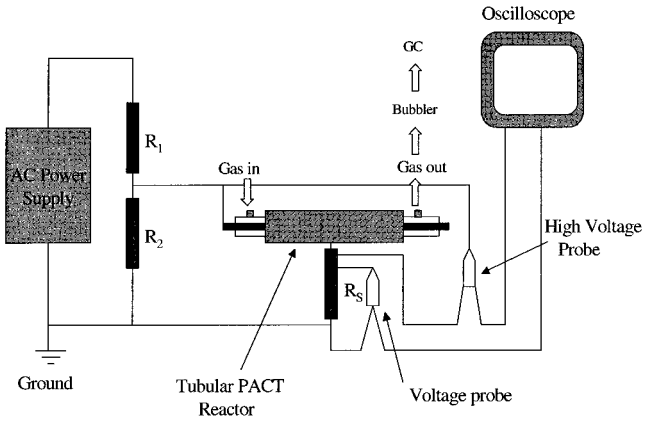

Figure 1. Schematic of the experimental setup for plasma generation and monitoring voltage and current conditions.

Experimental Setup and Parameters. A schematic of the experimental setup used is shown in Figure 1. The voltage to operate the tubular plasma reactor was produced by a Japan-Inter UHV-10 ac high-voltage generator with an operating frequency of between 8.0 and 8.1 kHz. Input voltage and input current values were measured by using a Tektronix 6015A high-voltage probe connected to a Yokogawa digital oscilloscope DL1520, in some cases a HV 15 HF 15 kV DC and Peak-to-Peak AC probe was used. The measurement of the input voltage required an additional voltage probe. The voltage measured across a 100 Ω resistor placed in series was used to monitor the input current. The other two resistors were placed before (R_1), and parallel to the tubular reactor (R_2). AC voltage values between 1.000 and 5.440 kV were applied to the electrodes to produce plasmas. The reactions were carried out at room temperature and atmospheric pressure by mixing Freon in helium and oxygen in helium (moisture added if needed) online to achieve a 0.5% concentration of Freon and 5% of oxygen, respectively, while using flow rates of 20 up to 80 mL/min. To prevent damage to the GC, a water bubbler was installed to trap the produced HF and HCl, and a subsequent water trap.

Product Analysis. The reaction products were analyzed using a Hewlett-Packard 5890 Series II gas chromatograph (GC) employing a thermal conductivity detector (TCD). The columns used were an Alltech Poropak N 80/100 column (6 ft × 1/8 in. × 0.085 in. i.d. stainless steel) for the Freon analysis, and a Supelco 45/60 Carboxen 1000 (5 ft × 1/8 in. stainless steel) for the carbon monoxide/carbon dioxide analysis. The disappearing Freon peak achieved with the Poropak N column was monitored to determine conversion. To measure the yield of CO_2 the corresponding peak was analyzed and compared with a calibration. In the case of the Carboxen column the conversion was measured as the appearance of CO_2. The ratio of CO to CO_2 is the ratio of the corresponding areas. The calibration of the columns for CO_2 was done with mixtures prepared in the lab.

Mass spectroscopic studies were carried out using an MKS-UTI PPT quadrupole residual gas analyzer mass spectrometer with a Faraday cup detector and a variable high-pressure sampling manifold. The *m*/*z* range achievable lies between 0 and 200 *m*/*z* units.

Plasma Diagnostics. Plasma diagnosis was done using a 270 M SPEX optical emission spectrometer with a liquid nitrogen cooled charge-coupled device (CCD). Emission spectra were recorded at wavelengths of 200−900 nm. A slightly modified setup was used. A quartz tube has to be used as the reaction tube because it yields better optical emission data. Three holes

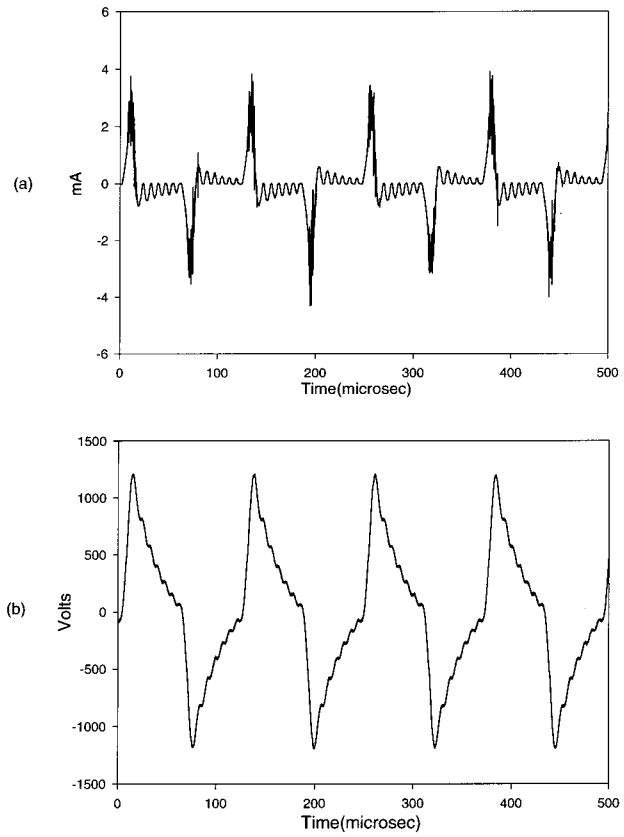

Figure 2. (a) Current and (b) voltage vs time waveform for the closed circuit plasma conditions for 0.5% Freon 21 and 5.0% oxygen in He mixture in an Fe reactor.

were drilled into the aluminum foil, one in the front part, one in the middle, and one at the end of the plasma zone. The emitted light from the plasma was collected at these holes and transported by a fiber optic cable to the monochromator.

Results

Voltage and Current Characterization of the Plasma. Typical voltage data from the oscilloscope are shown in Figure 2. Data for the closed circuit at plasma conditions are shown in Figure 2b. As the voltage is switched on with the reactor in the circuit it is observed that a certain voltage is necessary to achieve plasma conditions. In the case of Freon 21 a voltage of over 1.60 kV was desired at a concentration of 0.5% and of over 1.020 kV at a concentration of 0.1%. During the initiation period the shape of the voltage curve keeps building up until reaching a steady value after about 30 s. The final shape of the resulting curve for the closed circuit is closely related to the shape of the input voltage curve. The power supply does not produce a perfect sin wave as seen in the resulting waveform.

The current wave, measured as an averaged voltage wave, is in phase with the voltage wave, see Figure 2a. The current wave (averaged) goes down relatively sharply from the maximum, wiggles around the zero value, and then drops to the minimum. The nonaveraged current curve showed a different behavior. The waveform oscillates and shows maxima and minima where the voltage wave has its maxima and minima. Furthermore, depending on conditions, up to two maxima are observed in voltage.

Destruction of Freons. The destruction of Freons was studied using just one reactor setup, with an iron inner electrode and either copper or aluminum as the outer electrode. Effects of input voltage, flow rate, and the addition of water and oxygen were studied.

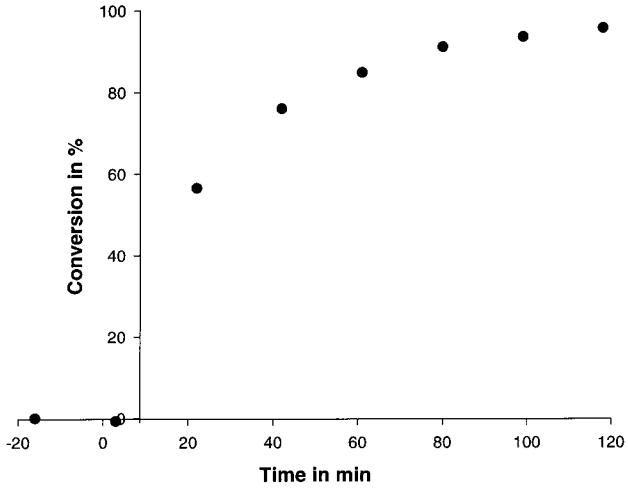

Figure 3. Destruction of 0.5% Freon 21 in 5.0% oxygen and He at 19.4 mL/min and $V_{p-p} = 2.560$ kV.

These studies focused on reactions with 0.5% Freon 21 as the probe gas, but also reactions with 0.1% Freon 21 and 0.25% Freon 142 B were carried out. The probe gas was mixed online in a 1:1 ratio with respect to flow rate with helium, oxygen in helium, or oxygen and water in helium. Prior to the reaction, an equilibrium time of 1.5−2 h is desired and checked by a constant area count on the GC. The reaction itself usually took about 2 h. An equilibrium state was also desired at the end of the reaction. Therefore, the run was sometimes prolonged accordingly or aborted if no Freon peak was present.

The data collected for the three different conditions at constant flow rate show similar trends. A sharp rise in conversion was observed over the first 20−40 min of the reaction. The conversion then leveled off for the remaining time until reaching equilibrium. The conversion data differ in the time equilibrium was reached and also in the equilibrium conversion value.

In the case of Freon 21 mixed with oxygen in helium, the usual behavior was observed with respect to conversion as seen in Figure 3. After the equilibration period, the conversion rises to 60−70% conversion over the first 40 min and levels off at about 95% after about 120−140 min. If the conversion data for several different voltages are plotted against time (Figure 4), the conversion of Freon 21 above a certain threshold input voltage is independent of the applied input voltage and follows the same trend from this low voltage up to higher voltages.

When Freon is used by itself at a concentration of 0.5% in helium, the conversion results are different. The conversion follows the same trend over the first period of the reaction. The difference is that some dependence of the final conversion on the applied input voltage is observed. The upper limit for a conversion of 95% is the same as in the previous case (Figure 5). The lower limit is 75% for applied input voltages of 1.700 kV and higher with the same barrier input voltage of 1.600 kV.

Furthermore, a different Freon 21 concentration of 0.1% in helium was used (Figure 6). The conversion is similar to the one with a 0.5% concentration of Freon 21. The only difference with respect to these data is that conversion of 100% is achievable and the lower limit is 80% above the barrier voltage. The barrier input voltage of 1.020 kV in this case is clearly lower than that for the higher Freon concentration.

The addition of water to a mixture of 0.5% Freon and 5% oxygen does not seem to have a detrimental effect on the conversion of Freon 21 (Figure 7). The conversion is as high

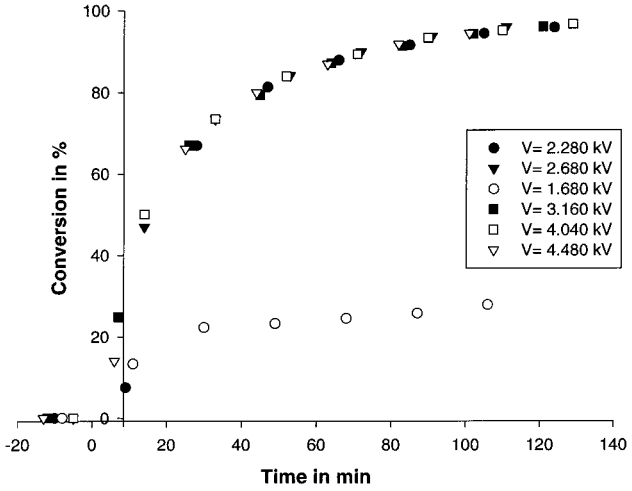

Figure 4. Destruction of 0.5% Freon 21 in 5.0% oxygen and He at 20 mL/min and variable input voltage.

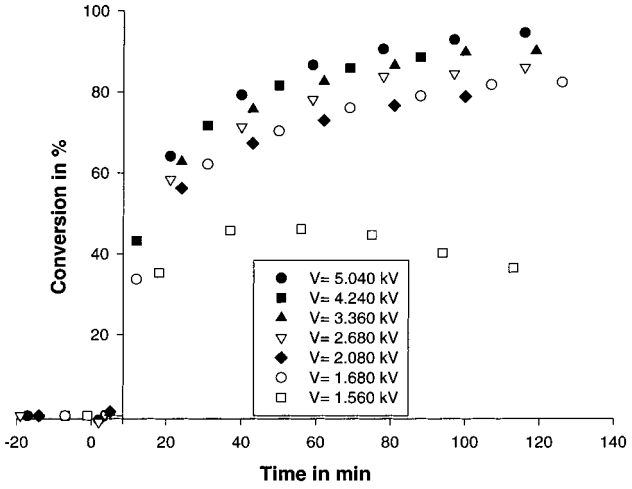

Figure 5. Destruction of 0.5% Freon 21 in He at 20 mL/min and variable input voltage.

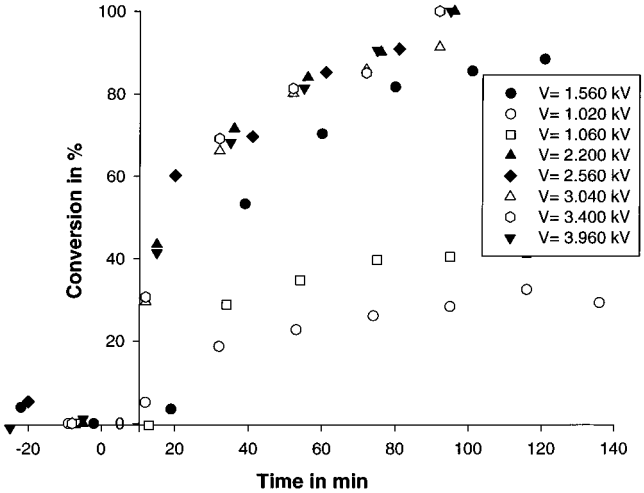

Figure 6. Destruction of 0.1% Freon 21 in He at 20 mL/min and variable input voltage.

as in the other cases at the same Freon concentration. Furthermore, the barrier input voltage of 1.60 kV is similar to the before-mentioned cases. The effect of the flow rate on conversion was studied in this case showing a dependence on flow rate as expected (Figure 8). At low flow rates the conversion is high (88% at 15 mL/min), decreases to 78% at 40 mL/min,

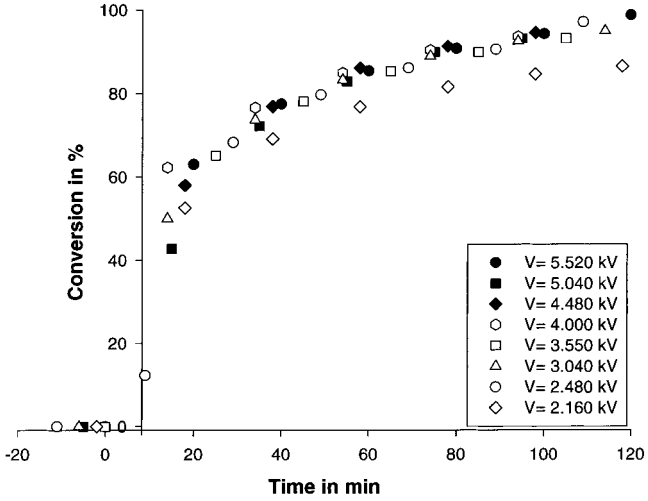

Figure 7. Destruction of 0.5% Freon 21 in 5.0% oxygen/water and He at 20 mL/min and variable input voltage.

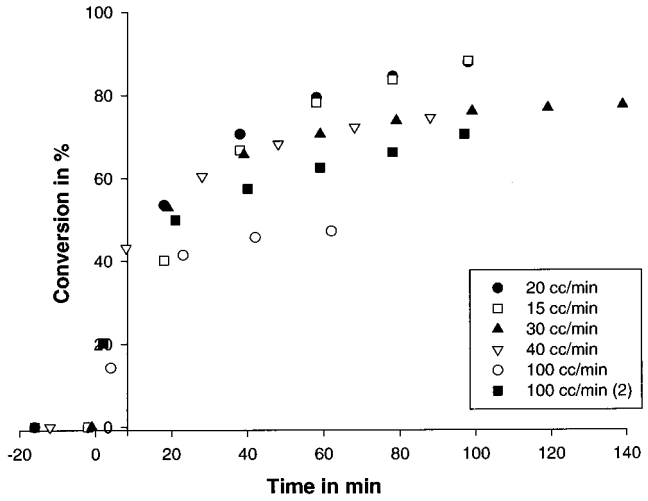

Figure 8. Destruction of 0.5% Freon 21 in 5.0% oxygen/water and He at $V_{p-p} = 2.440$ kV mL/min and variable flow rates.

and is even lower at high flow rates (47% at 100 mL/min). An interesting observation is that at 100 mL/min the conversion increases if water is omitted from the feed.

The flow rate also showed some effect on CO_2 production. At a higher voltage (3.440 kV), conversion decreases by 30% when the flow rate is changed from 20 to 40 mL/min and by 42% if changed to 60 mL/min. The selectivity to CO_2 is a parameter that is more directly influenced by the admixture of oxygen or oxygen and water to the Freon species (Figure 9). In the case of just the Freon species only traces of oxygen are present in the reaction system and only small amounts of CO_2 are formed. If oxygen is introduced, CO_2 production increases by 90% compared to the oxygen-deficient case and the admixture of water, additional to oxygen, increases this value by another 25%. Furthermore, CO_2 is the main carbon oxide as seen at a CO/CO_2 ratio of 0.05 to 0.07, and by earlier data showing that CO_2 shows selectivity up to 95% depending on input voltage.

A few experiments were carried out with Freon 142B yielding only qualitative conclusions (Figure 10). The conversion increases with increasing input voltage, but the increase seems more linear than in the case of Freon 21 where it was more exponential with oxygen and water admixed. This could also be due to the lack of data points. The selectivity to CO_2 shows the same trend as the conversion and reaches almost 100%.

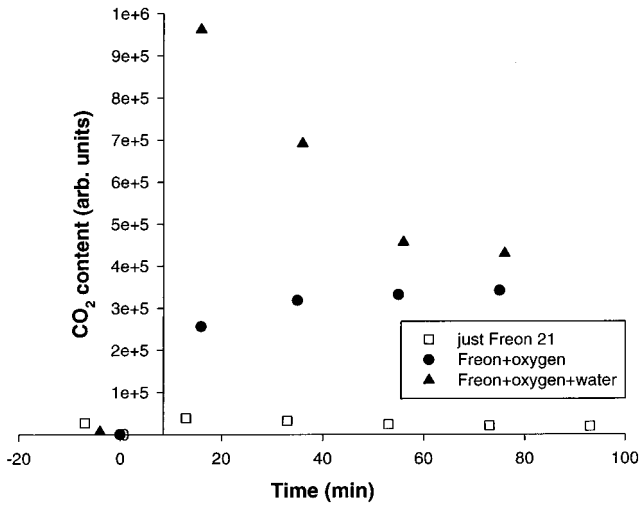

Figure 9. CO_2 production from 0.5% Freon 21 in 5.0% oxygen/water and He at 20 mL/min and $V_{p-p} = 3.440$ kV mL/min.

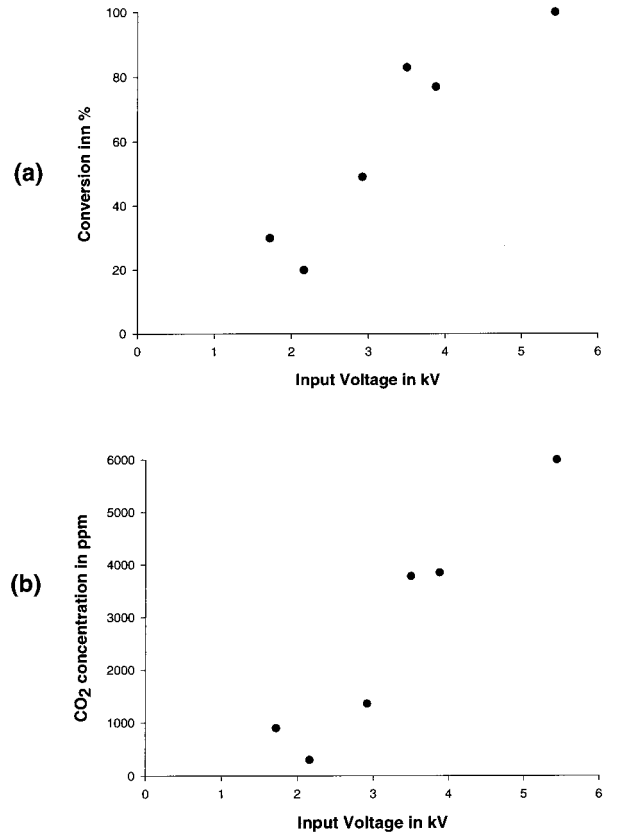

Figure 10. Destruction of 0.5% Freon 142B in 5.0% oxygen/water and He and CO_2 production at variable voltage and 20 mL/min.

Studies at other conditions of Freon or Freon with oxygen were not carried out.

Optical Emission Studies. To get insight into the mechanism of different plasma reactions involving Freons, optical emission studies were carried out. In these studies several different mixtures of two Freons with or without oxygen and with and without water in helium and helium by itself were analyzed using this method.

Their respective spectra were taken at total flow rates of 20 mL/min and identical voltage conditions at the maximum achievable voltage of about 5.5 kV. Three sets of data were taken for these two Freons at all three observation holes in the plasma zone. Additionally, background spectra for pure helium were collected at all three holes for comparison.

The background spectrum contains several characteristic lines with the helium line at 706.5 nm being by far strongest (Figure 11a).[23] Other strong characteristic helium lines are observed at 587.6, 667.6, and 728.2 nm, as well as a line of He^+ at 656.3 nm.[23] Strong lines of oxygen radicals ($O^\bullet$) are found at 777.2 and 844.64 nm.[23] The nitrogen lines are mainly due to the weaker first positive system of N_2 ($B^3\Pi_g$-$A^3\Sigma_u^+$) at 639.8 nm, and the stronger first negative system of N_2^+ ($B^2\Sigma_u^+$-$X^2\Sigma_g^+$) at 391.2 nm, and 427.6 nm.[24] Other very weak signals were observed and might be attributed to OH and H_2O^+. The spectra taken at the three holes are identical with hole #1 being the most intense one and hole #2 being least intense. Lines of He_2 and He_2^+ are absent in these spectra. The lines of oxygen and nitrogen species are most likely caused by discharge of air between the CCD detector tip and the foil surrounding the hole where the spectra are taken.

When Freon 142B is introduced into the system the spectra changed dramatically as seen in intensity drop by about 75% of the main helium line (Figure 11b). The intensities of other helium lines also decreased, down 35% for the line at 667.8 nm to 58% down for the one at 728.2 nm, whereas the intensity of the He^+ line at 656.3 nm more than doubled. All the nitrogen and oxygen peaks disappeared. The described changes in the helium lines show that the interactions between the different states of helium and the Freon molecules are of different strength. Due to the low Freon concentration (2500 ppm) and the strength of their transitions the additional lines that appear are relatively weak. Peaks of fluorine radicals are seen between 730 and 760 nm with the major ones being at 740.0 and 733.3 nm, and minor ones at 742.7, 755.3, and 757.3 nm.[23] A system of fluorine bands can be observed around 430 nm with the species being F^+ and F_2^+.[23,24] Furthermore, a weak signal of CH ($A^2\Delta$-$X^2\Pi$) can be seen at 431.0 nm which maybe coincides with F_2^+.[24] This signal was only seen in holes #1 and #2, but it is the most intense in hole #1. Several transitions of the hydrogen radical are present as well located at 433.8 nm (weak), 486.1 nm (medium), and 656.2 nm (strong).[23] This could be the reason the peak at this wavelength, which coincides with He^+, increased in intensity because one molecule of Freon 142B could yield three hydrogen radicals. Further analysis of the multi-line system between 425 and 435 nm showed lines of C^+ or $Cl^\bullet$ at 426.6 nm, F^+ at 427.8 and 430.0 nm, F_2^+ at 428−430 nm, and C^{2+} at 432.7 nm.[23,24] There are still some more peaks which could not be assigned. Data from hole #3 showed only two peaks, one at 427.6 which could be F^+ and an unidentified line at 431.7 nm. Signals of chlorine radicals were found at wavelengths of 774.5, 808.8, and 837.6 nm. The latter two were the more intense ones. No lines of C_2, CF, CF_2, Cl_2, HF, or F_2 were observed.

The further addition of oxygen (5%) to this Freon/helium system caused more drastic changes in these spectra (Figure 11c). The helium peaks are further reduced in intensity, some by up to 85% (705.6 nm); others are reduced by 30−50%. Weak lines of oxygen radicals due to the addition of oxygen are observed at 777.2 and 846.6 nm. The hydrogen lines are still present due to the CH content but they are reduced (as seen in the peak at 656.6 nm which coincides with the one of He^+). The observed lines of fluorine and chlorine radicals and CH are absent in these spectra. The reduction in line intensity agrees well with earlier observations that the addition of oxygen into helium systems drastically decreases the intensity of helium lines.[25] The addition of water vapor to this system resulted in no significant changes in the spectra (Figure 11d). The intensities of the helium peaks are slightly higher and the oxygen radical

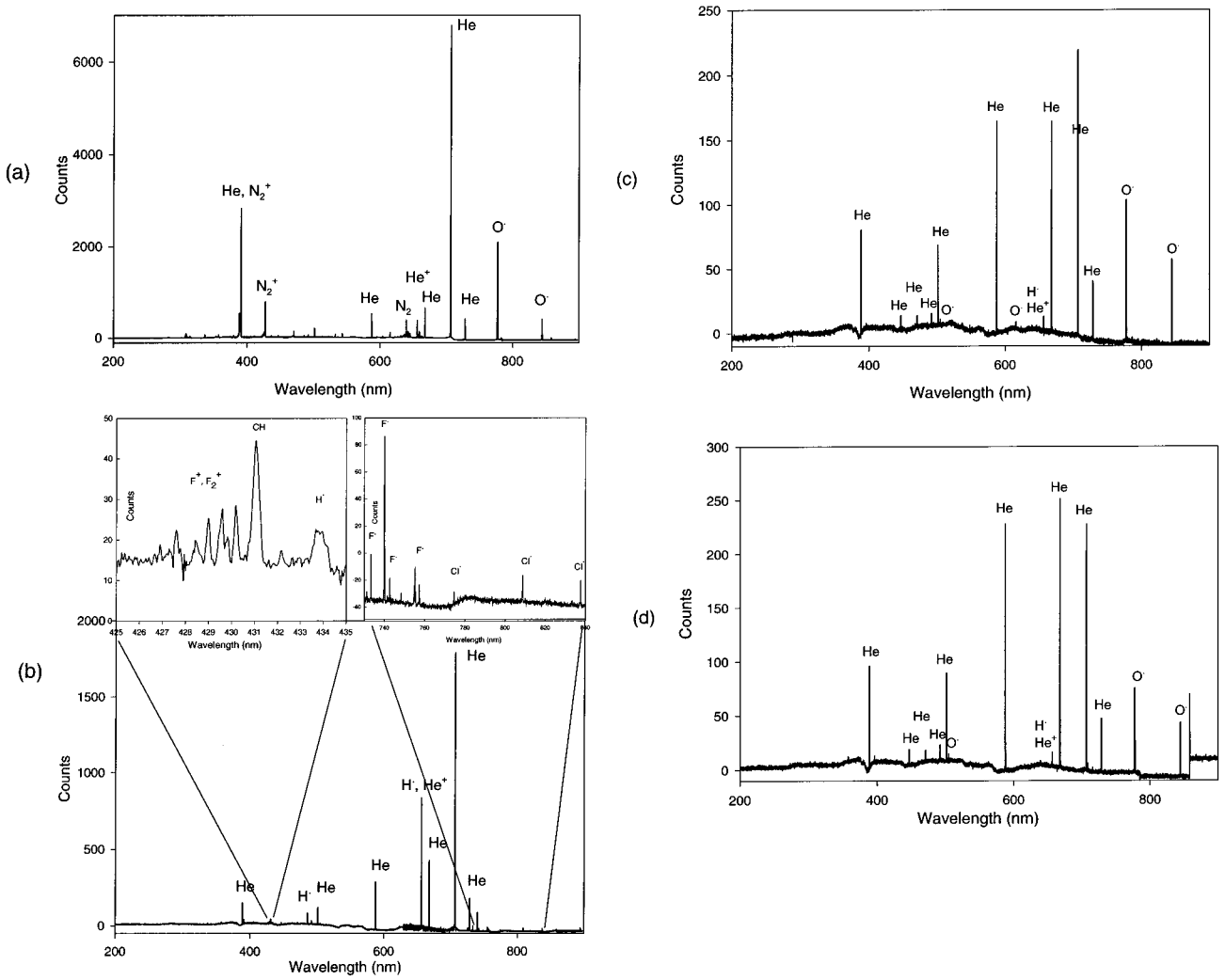

Figure 11. OEM spectra of (a) pure He, (b) 0.25% Freon 142B in He, (c) 5% O_2 and 0.25% Freon 142B in He, and (d) 5% O_2 and 0.25% Freon 142B in He with H_2O at 20 cm^3/min flow rate and 5.6 kV.

peaks are slightly lower. The hydrogen lines seem to have the same intensity as before, despite the addition of water. The line at 706.5 nm is no longer the strongest line; the most intense transition is at 667.6 nm. This is due to different interactions of the carrier gas and the other gases. The presence of OH radicals is debatable because the peaks cannot be clearly distinguished from the background.

These experiments were also done with a mixture of 0.5% Freon 21 in helium (Figure 12a). These spectra show the same trends as observed in the spectra of Freon 142B. Peaks of chlorine, fluorine, hydrogen radicals, CH, two fluorine species (F^+ and F_2^+), and two carbon species (C^+ and C^{2+}) appear upon Freon addition. The only difference from the Freon 142B spectra lies in the intensities. These systems are more prominent and more refined for Freon 21. Due to higher intensity of the CH transitions a second ($C^2\Sigma^+$-$X^2\Pi$ at 314.5 nm) and third CH transition ($B^2\Sigma$-$X^2\Pi$ at 387.0 nm) can be observed. The hydrogen line at 656.6 nm (coinciding with He^+) seems to be lower in intensity since one molecule of Freon 21 could just yield one hydrogen radical. Data collected at hole #3 (not shown) have a relatively high intensity. The addition of oxygen and then water had the same effect as in the spectra of Freon 142 B (Figure 12a,b). The observed lines of the fluorine and chlorine radicals and CH disappear. The oxygen radical lines are still present, and the hydrogen system is still unchanged after water addition.

Mass Spectroscopic Studies. These studies were done to determine products in the case of a Freon/helium plasma. Three mass spectra are shown in Figure 13, the first two are background spectra for helium and Freon (1.0%) in helium, respectively; the third is a spectrum of the species after plasma conditions. The helium background spectrum shows traces of water, nitrogen, oxygen, and CO_2 due to residues in the lines from the reactor to the mass spectrometer. The helium peak itself was removed due to its very high intensity. The spectrum of Freon 21 agrees well with the literature.[26] By comparing the last two spectra, Freon 21 is clearly destroyed and new species are formed. It is not easy to determine the exact nature of the new species because this spectrum is a convolution of several spectra of the products and Freon 21 with different weights. The resulting new peaks can be qualitatively assigned to several different species by comparison with literature spectra.[26] Freon 21 seems to be dissociated by about 87%, which is in good agreement with previously discussed gas chromatography data (Figure 13c). The actual conversion should be higher because the products of the decomposition overlap with the molecular peak at this *m*/*z* ratio. The major new peaks are the ones at *m*/*z* of 51, 85 and 87, 101 and 103, and a series of peaks at and above 117.

The destruction of Freon 21 seems to favor the evolution of chlorine rich species which is in contrast to previously mentioned work by Stoffels[16] where fluorine-rich species were

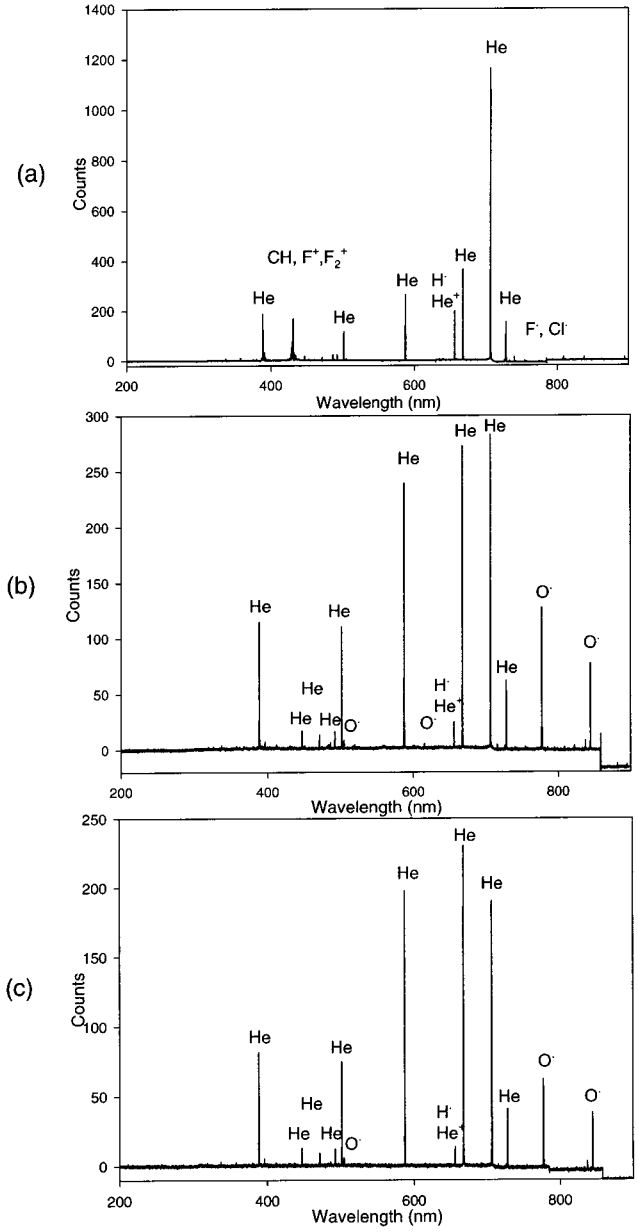

Figure 12. OEM spectra of (a) 0.5% Freon 21 in He, (b) 5% O_2 and 0.5% Freon 21 in He, and (c) 5% O_2 and 0.5% Freon 21 in He with H_2O at 20 cm^3/min flow rate and 5.6 kV.

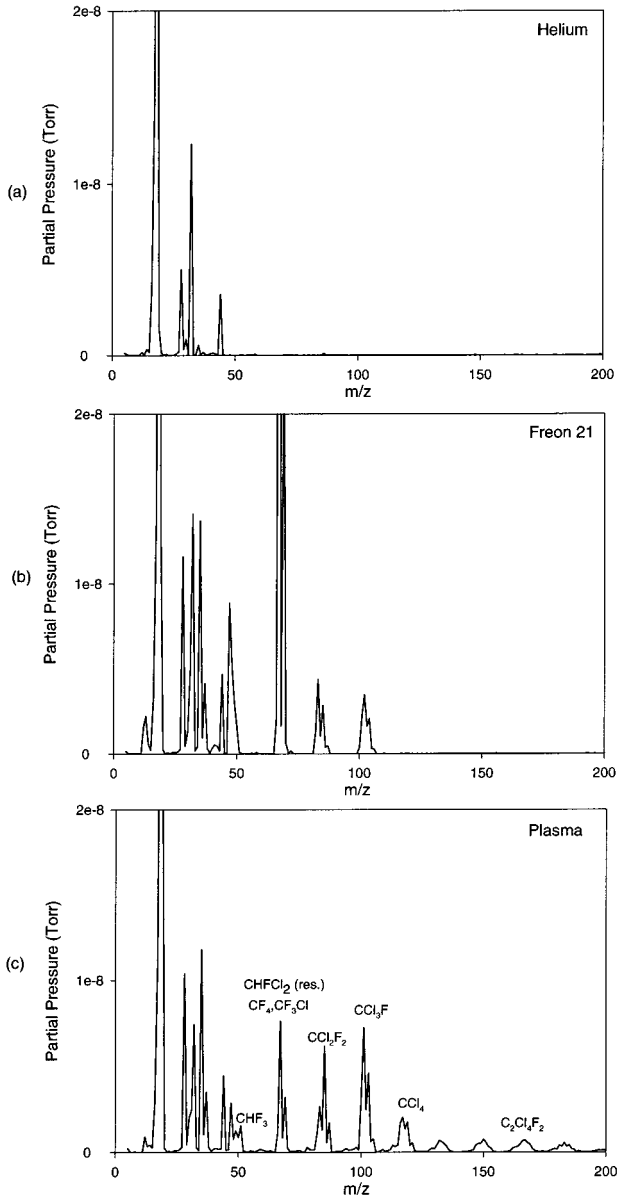

Figure 13. Mass spectra of (a) pure He, (b) 1.0% Freon 21 in He before reaction, and (c) 1.0% Freon 21 in He under plasma conditions.

favored at low-pressure conditions (0−400 mTorr). The pair with *m*/*z* of 101 and 103 represents CCl_3F and has a selectivity of about 12% considering that only this molecule contributes to these peaks. The other pair of peaks at 85 and 87 can be assigned to CCl_2F_2 with a selectivity of about 10%. Furthermore, the peaks at 51, 69, and 117 can be assigned to CHF_3, CF_4, and CF_3Cl, and CCl_4, respectively. The peak at 51 is likely to be CHF_3 because others with a peak at 51 do not have the other corresponding peaks. CF_4 and CF_3Cl must be part of the peak at 69 because the ratio of 69 to 67 is too high for just being from Freon 21. The peaks from 117 onward are likely to be C2s and C3s such as 1,1,2,2-tetrachloro-1,2-difluoroethane. Some of these must also have a peak at *m*/*z* of 102 because the abundance for this ion is too high. This peak shows a conversion of 28%, which is not as high as observed for the molecular ion at *m*/*z* of 67, which is 87%.

Some trends regarding the formation of small fluorine- and chlorine-containing molecules can be drawn from the mass spectrometry data. Comparison of the data of masses 19 and 38 at plasma conditions and before reaction indicates formation of hydrogen fluoride and no formation of fluorine, as seen in the increasing peak at mass 19 under plasma conditions and the decreasing peak at mass 38. The decrease in the peaks at masses 35, 37, and 70 indicate no formation of hydrogen chloride and chlorine.

Power and Efficiency Measurements. The power used in reactions was calculated by integration of voltage versus current curves. The method for integration used the trapezoid rule. These calculations were carried out using Sigma Plot 3.0. If the power is plotted against the applied input voltage, the best fit is a straight line with an intersect at about 1.60 kV. This is the barrier voltage for most cases for Freon 21 at a concentration of 0.5% (Figure 14).

Sets of the data for the case involving oxygen and Freon 21 in helium and one for just Freon 21 in helium were used to calculate the efficiency of these reactions. Data for these calculations are listed in Tables 1 and 2.[27] In eq 1, *F* represents the flow rate in mL/s, C_0 the Freon concentration in volume % used, χ the conversion in %, *P* the power consumed in W, 22400

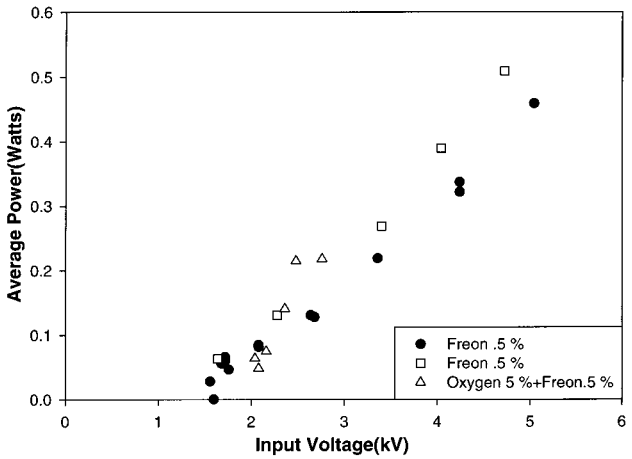

Figure 14. Correlation of average power to input voltage for 0.5% Freon 21 in He and 0.5% Freon 21 in 5.0% oxygen and He.

TABLE 1: Efficiency as a Function of Flow Rate, Percent Conversion, and Power at a Concentration of Freon 21 of 0.5% and Oxygen of 5.0% in Helium and Different input voltages (V_{in})

V_{in} (kV)	power (W)	conversion (%)	flow rate (mL/min)	efficiency (mol/J)
2.040	0.0640	100	20.1	1.08×10^{-6}
2.080	0.0484	100	19.9	1.42×10^{-6}
2.160	0.0750	100	20.1	9.20×10^{-7}
2.360	0.141	100	20.0	4.90×10^{-7}
2.480	0.215	100	20.0	3.20×10^{-7}
2.760	0.218	100	20.1	3.17×10^{-7}

TABLE 2: Efficiency as a Function of Flow Rate, Percent Conversion, and Power at a Concentration of Freon 21 of 0.5% in Helium and Different Input Voltages (V_{in})

V_{in} (kV)	power (W)	conversion (%)	flow rate (mL/min)	efficiency (mol/J)
1.640	0.0634	76	20.0	8.29×10^{-7}
2.280	0.131	83	20.0	4.38×10^{-7}
3.400	0.269	95	20.0	2.44×10^{-7}
4.040	0.390	93	20.0	1.65×10^{-7}
4.720	0.509	100	20.0	1.36×10^{-7}

mL/mol the molar volume at 273 K, 0.93 the correction factor for the molar volume from 273 to 298 K:

$$\text{efficiency (in mol/}J) = (0.93 \times F \times C_0 \times \chi)/(1\ \text{s} \times 22400 \times P) \quad (1)$$

The efficiency of these reactions is fairly low with about 1.0×10^{-6} mol/J. The efficiency itself decreases by an order of magnitude with increasing power while increasing the input voltage from 1.640 to 4.720 kV in the case of Freon 21 by itself, but this trend is seen in the mixture with oxygen as well. In this mixture, the efficiency is slightly higher than for Freon 21 alone, as seen at about 2.3 kV where the Freon case shows an efficiency of 4.38×10^{-7} mol/J compared to 4.90×10^{-7} mol/J for Freon and oxygen.

Thermodynamic calculations of the total oxidation of Freon 21 showed that oxidation with oxygen alone is favored over the oxidation involving water vapor and oxygen as obtained from calculations of ΔH^0 and $\Delta G°$ for both scenarios. The reaction involving oxygen has $\Delta H° = -383.55$ kJ/mol and $\Delta G° = -416.93$ kJ/mol, compared to $\Delta H° = -234.05$ kJ/mol and $\Delta G° = -286.62$ kJ/mol for reaction without oxygen. Furthermore, this means that chlorine is thermodynamically favored over hydrogen chloride as a product.

Long-Term Stability. The stability of the iron electrode depends on the reaction conditions. If water is used in these reactions, the electrode and the glass tube have to be cleaned after at least 2 days. If oxygen is in the reaction mixture, rust is the only major problem, and the electrode lasts at least a week. Freon by itself does not impact the electrode performance. The influence on the glass tube is that it becomes "blind" due to the formation of silica or reaction with produced hydrogen fluoride. The iron electrode can be cleaned by using sandpaper, and the glass tube is rinsed with water first and then with acetone to remove residues. A component that has to be exchanged from time to time is the NUPRO filter (7 μm pore diameter), which is placed in line before the GC to prevent damage to the instrument.

Discussion

Activation of the Freon Molecules. The glow discharge plasmas used in these experiments are nonequilibrium plasmas at atmospheric pressure where real gas temperature is close to room temperature whereas the electronic temperature is on the order of several thousand Kelvin. This is caused by the nature of activation. The electric field accelerates the electrons to a certain speed and therefore gives them a certain energy. All species in the plasma are consequently not thermally activated but activated by high-energy electrons directly or indirectly.[28] The optical emission data suggest that the Freon molecules such as others (water and oxygen) are activated indirectly by excited helium species. This is in good agreement with a paper published recently by Luo et al.,[25] which states this as the major source of reactant molecule activation.

The optical emission work presented here encompasses reactions of two similar Freon molecules which readily react in the discharge plasma with the excited helium atoms and ions. The spectra of just helium as well as others show several different excited states of helium. The most important excited state in the activation of the Freon molecules is the 3^3S state with a line at 706.5 nm.[29] This line showed the biggest intensity drop upon Freon addition exhibiting the best energy transfer efficiency. Other helium lines show similar behavior but the efficiency is smaller. The decreases of efficiencies are as follows: He 3^3S (706.5 nm) > He 3^1S (728.2 nm) > He 3^3D (587.6 nm) > He 3^1D (667.8 nm) $\gg$ He^+ (656.3 nm). The assignment of the He^+ line poses a problem due to its overlap with an H· line. The extent to which each line contributes to the final line is unknown. Similar trends are observed when oxygen is added to the Freon/helium system. The extent to which the peaks are reduced is similar to the addition of Freon resulting in the same order of the excited states. Upon addition of water to the system the interactions of the molecules present are slightly weaker as seen in the stronger helium lines compared to the system without water due to interactions of oxygen with water.

Model for Decomposition. The model in Scheme 1 is valid for the decomposition of Freon 21 without oxygen or water and is pieced together from optical emission and mass spectrometry data with consideration of thermodynamic data (bond strengths).[23] The observed species of C^+, C^{2+}, F^+, and F_2^+ can be explained by electron abstraction of species formed in reactions 1−20. Small molecules containing fluorine and chloride like hydrogen fluoride are formed by reactions 9−13. Hydrogen fluoride is the major species formed under plasma conditions as seen in trends from the mass spectrometry data, whereas hydrogen chloride and fluorine do not seem to play a major role under these conditions. C2s, C3s, and higher hydrocarbons can be

SCHEME 1: Reaction Scheme for the Decomposition of Freon 21, Reactions 1−8 Show the Model without Water or Oxygen, Reactions 9−19 Show the Recombination Possibilities, and Reactions 20−30 Represent Additions to the Model with Water and Oxygen Added

$CHFCl_2 + He^* \rightarrow CHFCl_2^* + He$ (1)

$CHFCl_2^* \rightarrow CHFCl^\cdot + Cl^\cdot$ (2 a)

$CHFCl_2^* \rightarrow CFCl_2^\cdot + H^\cdot$ (2 b) **(minor)**

$CHFCl^\cdot + He^* \rightarrow CHFCl^{\cdot *} + He$ (3)

$CHFCl^{\cdot *} \rightarrow CHF^\cdot + Cl^\cdot$ (4 a)

$CHFCl^{\cdot *} \rightarrow CFCl^\cdot + H^\cdot$ (4 b)

$CHF^\cdot + He^* \rightarrow CHF^{\cdot *} + He$ (5 a)

$CFCl^\cdot + He^* \rightarrow CFCl^{\cdot *} + He$ (5 b) **(minor)**

$CHF^{\cdot *} \rightarrow CH^\cdot + F^\cdot$ (6 aa)

$CHF^{\cdot *} \rightarrow CF^\cdot + H^\cdot$ (6 ab)

$CFCl^{\cdot *} \rightarrow CF^\cdot + Cl^\cdot$ (6 ba) **(minor)**

$CFCl^{\cdot *} \rightarrow CCl^\cdot + F^\cdot$ (6 bb) **(minor)**

$CF^\cdot + He^* \rightarrow CF^{\cdot *} + He$ (7 a)

$CH^\cdot + He^* \rightarrow CH^{\cdot *} + He$ (7 b)

$CF^{\cdot *} \rightarrow C^\cdot + F^\cdot$ (8 a)

$CH^{\cdot *} \rightarrow C^\cdot + H^\cdot$ (8 b)

Recombination:

$H^\cdot + F^\cdot \rightarrow HF$ (9)

$F^\cdot + F^\cdot \rightarrow F_2$ (10)

$H^\cdot + Cl^\cdot \rightarrow HCl$ (11)

$Cl^\cdot + Cl^\cdot \rightarrow Cl_2$ (12)

$H^\cdot + H^\cdot \rightarrow H_2$ (13)

$CFCl_2^\cdot + CFCl_2^\cdot \rightarrow C_2F_2Cl_2$ (14)

$CHF + F_2 \rightarrow CHF_3$ (15)

$CFCl_2 + F^\cdot \rightarrow CF_2Cl_2$ (16)

$CFCl_2 + Cl^\cdot \rightarrow CFCl_3$ (17)

$CF^\cdot + F^\cdot + F_2 \rightarrow CF_4$ (18)

$CFCl^\cdot + F_2 \rightarrow CF_3Cl$ (19)

$CCl^\cdot + Cl^\cdot + Cl_2 \rightarrow CCl_4$ (20)

$O_2 + He^* \rightarrow O_2^* + He$ (21)

$O_2^* \rightarrow O^\cdot + O^\cdot$ (22)

$CH^\cdot + O^\cdot \rightarrow CO^\cdot + H^\cdot$ (23)

$CO^\cdot + O^\cdot \rightarrow CO_2$ (24)

$H_2O + He^* \rightarrow H_2O^* + He$ (25)

$H_2O^* \rightarrow OH^\cdot + H^\cdot$ (26)

$CH^\cdot + OH^\cdot \rightarrow CO + H_2$ (27)

$CO + OH^\cdot \rightarrow CO_2 + H^\cdot$ (28)

$F^\cdot + OH^\cdot \rightarrow O^\cdot + HF$ (29)

$Cl^\cdot + OH^\cdot \rightarrow O^\cdot + HCl$ (30)

formed by radical recombination; the evolution of substituted methane analogues and C2s such as $CFCl_2$, as observed in the mass spectra of Freon 21 under plasma conditions, are well documented by reactions 14−20. The formation of fluorinated aromatic compounds by radical recombination was confirmed by NMR analysis of the residue on the iron electrode (results are not shown in this paper).

Freon 142B follows a similar reaction scheme. In this case the abstraction of a hydrogen radical is substituted by abstraction of a methyl radical. The only pathway for the formation of hydrogen and CH radicals is the stepwise breakup of methyl radicals. The higher hydrogen content in Freon 142B explains the more intense hydrogen lines in the spectra of this Freon. The lower intensity for the CH line is due to the stepwise disintegration of methyl radicals resulting in lower probability of CH generation. The formation of fluorine compounds seems favored due to the higher abundance of fluorine in Freon 142B compared to Freon 21. The same trends for the evolution of higher hydrocarbons should apply for Freon 142B but the likelihood of this should be greater than in the case of Freon 21 due to the presence of methyl radicals and other carbon containing radicals or fragments such as substituted ethyl radicals.

The model for the decomposition of Freon 21 has to be modified if oxygen and water are present in the feed gas. Upon addition of oxygen and in the second case of oxygen and water the reaction products change drastically due to the excess of these species. The principal model of reactions 1−8 is still valid under these conditions but has to be modified by reactions 20−30. Since no lines of species in the first reactions (eqs 1−8) are observed in the optical emission spectra it is assumed that these are very quickly scavenged by $O^\bullet$, $OH^\bullet$, and $H^\bullet$ as shown in reactions 23, 27, 29, and 30. The formation of CO and CO_2 in this system is explained by reactions 21−28. The excess of oxygen in the feed explains the appearance of $O^\bullet$. The formation of hydrocarbons cannot be ruled out, especially with the formation of a polymer-like film on the electrode.

Efficiency Considerations. Mass spectrometry and gas chromatography data for the destruction of both Freons show very high conversions up to 100%. This "efficient" destruction is caused by the influence of the plasma. The easy abstraction of chlorine or hydrogen radicals seems to be the main driving force to yield almost complete destruction of the Freon molecules. To be viable for industrial applications the reaction efficiencies with respect to energy input need to be optimized. The data of Tables 1 and 2 show that these reactions have low energy efficiency. The efficiency decreases with increasing voltage because more molecules have the proper energy for reaction but the collisions between the molecules are less selective and less efficient as is the case at lower voltage. The efficiency of the destruction is slightly higher in the case where oxygen is added. This may be due to the presence of abundant oxygen radicals.

Generally, plasmas are a good and efficient way to break down hydrocarbons, which was shown in earlier research in our group.[30] The difficulty with Freons is that they are very hard to decompose due to their stability. In further studies in this field, it was found that CF_4 is even harder to decompose (conversions being lower than 20% under the same conditions) than these Freons due to its increased stability.[31] To improve the efficiency of this method, parameters such as frequency, input voltage, and surface of the electrode can be altered to achieve increased efficiency. A "cleaning gas" might be used to purge the reactor after usage to increase efficiency.

Conclusions

Hydrochlorofluorocarbons (HCFCs) are a very important substitute for the more dangerous chlorofluorocarbons (CFCs). In coming years further restrictions are likely to be implemented

to phase out these substitutes. Therefore, effective ways to get rid of these pollutants are crucial. High-voltage glow plasmas are effective in destroying pollutant Freons at atmospheric pressure and at room temperature. In these reactions almost complete destruction was observed at low energy efficiencies. Based on mass spectrometry data and optical emission data a model for the destruction of Freon 21 and Freon 142B was proposed and is in line with the experimental data. The main products of the reactions depend on reaction conditions. If Freon is used by itself, hydrogen fluoride, chlorinated and fluorinated methane analogues are formed with other hydrocarbons such as C2s, C3s, and aromatic compounds evolving at the same time. In the presence of oxygen, hydrogen fluoride is still one of the main products but carbon dioxide is the other major product with good selectivity, with small amounts of carbon monoxide also forming. The presence of other hydrocarbons was not investigated, but it is likely that higher hydrocarbons form due to polymer-like coverage of the electrode. The data for addition of water are very similar to data for oxygen and Freon. In this case, the conversion seems almost independent of the applied input voltage. Therefore, good conversions are possible at low voltages with relatively high efficiencies employing Freon and oxygen. This system is very well suited for the very efficient destruction of Freons under various conditions employed in this research.

Acknowledgment. The authors thank JFCC and Planet Japan for support of this research. We also thank Jeff Rozak for assistance in the power measurements and reactor setup.

References and Notes

(1) Solomon, S. *Nature* **1990**, *347*, 347.
(2) Rowland, F. S.; Molina, M. J. *Rev. Geophys., Space Phys.* **1975**, *13*, 1.
(3) Molina, M. J.; Rowland, F. S. *Nature* **1974**, *249*, 810.
(4) Rowland, F. S. *Annu. Rev. Phys. Chem.* **1974**, *42*, 731.
(5) Ravishankara, A. R.; Turnipseed, A. A.; Jensen, N. R.; Barone, S.; Mills, M.; Howard, C. J.; Solomon, S. *Science* **1994**, *263*, 71.
(6) Solomon, S.; Albritton, D. L. *Nature* **1992**, *357*, 33.
(7) Hayman, G. D.; Derwent, R. G. *Environ. Sci. Technol.* **1997**, *31*, 327.
(8) *The UNEP Ozone Secretariat*, http://www.unep.org/ozone/, February **2000**.
(9) Vercammen, K. L. L.; Berezin, A. A.; Lox, F.; Chang, J. S. *J. Adv. Oxid. Technol.* **1992**, *2*, 312.
(10) Ruddy, E. N.; Caroll, L. A. *Chem. Eng. Prog.* **1993**, *89*, 28.
(11) Takita, Y.; Ishihara, T. *Catal. Surv. Jpn.* **1998**, *21*, 165.
(12) Sonoyama, N.; Sakata, T. *Environ. Sci. Technol.* **1998**, *32*, 375.
(13) Sonoyama, N.; Sakata, T. *Environ. Sci. Technol.* **1998**, *32*, 4005.
(14) Gritsinin, S. I.; Kossyi, I. A.; Nisakyan, M. A.; Silakov, V. P. *Plasma Phys. Rep.* **1997**, *23*, 242.
(15) Aleksandrov, N. L.; Dobkin, S. V.; Konchakov, A. M.; Novitskii, D. A. *Plasma Phys. Rep.* **1994**, *20*, 442.
(16) Stoffels, W. W.; Stoffels, E.; Haverlag, M.; Kroesen, G. M. W.; de Hoog, F. J. *J. Vac. Sci. Technol.* **1995**, *13*, 2058.
(17) Wang, Y.-F.; Lee, W.-J.; Chen, C.-Y.; Hsieh, L.-T. *Environ. Sci. Technol.* **1999**, *33*, 2234.
(18) Korzekwa, R. A.; Rosocha, L. A. *J. Adv. Oxid. Technol.* **1999**, *4*, 390.
(19) Oda, T.; Yamashita, R.; Tanaka, K.; Takahashi, T.; Masuda, S., *IEEE Trans. Ind. Appl.* **1996**, *32*, 1044.
(20) Oda, T.; Yamashita, R.; Takahashi, T.; Masuda, S. *IEEE Trans. 1nd. Appl.* **1996**, *32*, 227.
(21) Akhmedzhanov, R. A.; Vikharev, A. L.; Gorbachev, A. M.; Ivanov, O. A.; Kolysko, A. L. *High Temp.* **1997**, *35*, 524.
(22) Akhvlediani, Z. G.; Barkhudarov, E. M.; Gelashvili, G. V.; Kossyi, I. A.; Melitauri, I. T.; Taktakishvili, M. I. *Plasma Phys. Rep.* **1996**, *22*, 470.
(23) *CRC Handbook of Chemistry and Physics*, 75th ed.; Lide, D. R., Ed.; CRC Press: Boca Raton, FL, 1994; Section 10, 1−127.
(24) Pearse, R. W. B.; Gaydon, A. G. *Identification of Molecular Spectra*; Chapman and Hal: New York, 1976.
(25) Luo, J.; Suib, S. L.; Hayashi, Y.; Matsumoto, H. *J. Phys. Chem. A* **1999**, *103*, 6151−6161.
(26) Stein, S. E. *NIST Standard Reference Database* Number 69−November **1998** Release.
(27) Luo, J.; Suib, S. L.; Marquez, M.; Hayashi, Y.; Matsumoto, H. *J. Phys. Chem. A* **1998**, *102*, 7954.
(28) Dresvin, S. V. *Physics and Technology of Low-Temperature Plasma*; The Iowa State University Press: Ames, IA, 1977.
(29) Reader, J.; Corliss, C. H.; Wiese, W. L.; Martin, G. A. *Wavelengths and Transition Probabilities for Atoms and Atomic Ions*; Natl. Stand. Ref. Data Ser., Natl. Bur. Stand. (U.S.) **68**, 1980.
(30) Huang, A.; Xia, G. G.; Wang, J.; Suib, S. L.; Hayashi, Y.; Matsumoto, H. *J. Catal.* **2000**, *189*, 349−359.
(31) Spiess, F.-J.; Huang, A.; Chen, X.; Suib, S. L.; Takahshi, T.; Hayashi, Y.; Matsumoto, H. Manuscript in preparation.